EDORIUM Journals

J Case Rep Images Pathol 2023 Jul-Dec;9(2):5–13.
www.ijcripathology.com

CASE REPORT PEER REVIEWED | OPEN ACCESS

Desmoplastic small round cell tumor of the pleura with brain metastasis: A case report and literature review

Rebecca Phillips, Sumit Das

ABSTRACT

Introduction: Desmoplastic small round cell tumor (DSRCT) is a rare and aggressive mesenchymal neoplasm characterized by a chromosomal translocation involving the EWSR1 and WT1 genes. It typically arises in intra-abdominal tissues (i.e., mesentery, omentum, pelvic organs), and commonly spreads to regional lymph nodes, lungs, or liver, while central nervous system (CNS) metastasis is rare.

Case Report: We present a unique case of DSRCT originating from the pleura in a young female, which was metastatic to intrathoracic and mediastinal tissue at diagnosis and later spread to the brain. The initial tumor samples exhibited characteristic histopathological features, including small round cells with minimal cytoplasm and indistinct borders embedded in a fibroblastic stroma. Notably, the brain metastasis demonstrated distinct histological characteristics, lacking the desmoplastic stroma observed in previous biopsies.

Conclusion: This case underscores the diagnostic challenges associated with DSRCT, emphasizes the significance of early recognition and appropriate histological evaluation, and contributes to the limited literature on the histological features and metastatic behavior of this rare tumor.

Keywords: Brain, Central nervous system, Desmoplastic small round cell tumor, DSRCT, EWSR1

How to cite this article

Phillips R, Das S. Desmoplastic small round cell tumor of the pleura with brain metastasis: A case report and literature review. J Case Rep Images Pathol 2023;9(2):5–13.

Article ID: 100074Z11RP2023

****

doi: 10.5348/100074Z11RP2023CR

Rebecca Phillips[1], Sumit Das[2]

Affiliations: [1]MD, Anatomical Pathology resident, Department of Laboratory Medicine and Pathology, University of Alberta Hospital, Edmonton, Alberta, Canada; [2]MD, FRCPC, Neuropathologist, Department of Laboratory Medicine and Pathology, University of Alberta Hospital, Edmonton, Alberta, Canada.

Corresponding Author: Rebecca Phillips, Department of Laboratory Medicine and Pathology, University of Alberta, 5B2.19, Walter C. Mackenzie Centre, 8440-112 Street NW, Edmonton, Alberta T6G 2B7, Canada; Email: rphilli1@ualberta.ca

Received: 28 May 2023
Accepted: 11 July 2023
Published: 28 July 2023

INTRODUCTION

First described in 1989 by Gerald and Rosai [1], desmoplastic small round cell tumor (DSRCT) is an uncommon and aggressive mesenchymal neoplasm of uncertain differentiation. It is typified by a chromosomal translocation that fuses the EWSR1 gene (22q12) and the WT1 gene (11p13) [2]. Desmoplastic small round cell tumor mainly affects young males and classically arises in intra-abdominal tissues, where it may involve the retroperitoneum, omentum, pelvis, or mesentery; its common sites of metastasis include the regional lymph nodes, lungs, or liver [3]. Histopathologically, the tumor displays nested aggregates of small round cells with scant cytoplasm and indistinct borders, embedded in a fibroblastic or collagenized stroma [2]. Its primitive ultrastructural appearance and variable immunohistochemical expression suggest polyphenotypic differentiation, though it typically shows EMA, desmin (cytoplasmic, “dot-like”), and cytokeratin positivity [2, 4, 5]. Only rare examples of central nervous system metastasis have been reported. This report

presents an unusual case of a young female with DSRCT originating from the pleura, with local spread at diagnosis and subsequent brain metastasis. This rare tumor with an uncommon site of metastasis provides a valuable opportunity to contribute to the limited literature on the histological features and metastatic behavior of DSRCT.

CASE REPORT

A 20-year-old woman with no past medical history or tobacco use presented with dry cough and left-sided lower rib pain lasting six months. Physical examination and laboratory tests were unremarkable. However, chest X-ray revealed a 9.2 cm mass-like opacity in the left mid to lower lung zone, accompanied by a small pleural effusion.

A follow-up computed tomography (CT) scan identified a solid mass with central mineralization involving the left lower lobe and pleura; enlarged lymph nodes were found in the mediastinum (Figure 1). Positron emission tomography (PET) revealed the direct connection between the hypermetabolic mass and both the pleura and lung parenchyma. This finding caused difficulty in determining whether the pleura or the lung was the actual site of origin, which was resolved later with subsequent imaging as described below. In addition to the main mass, PET-avid metastatic foci were detected within multiple non-contiguous surfaces of the left pleura. No evidence of metastasis outside the thoracic region was found, and a magnetic resonance imaging (MRI) of the brain showed no abnormalities.

Biopsies of mediastinal lymph nodes and the left lung, performed using endobronchial ultrasound guidance, revealed densely cellular fragments of cells with round to ovoid nuclei and minimal cytoplasm. There was a proportionally smaller quantity of desmoplastic stromal tissue present (Figure 2). Ancillary study results are provided in Table 1. The biopsy was diagnosed as a poorly differentiated carcinoma with an inconclusive immunohistochemical staining pattern. Treatment was initiated for advanced-stage carcinoma presumed to be of bronchogenic origin, and the patient underwent palliative thoracic radiotherapy and chemotherapy (cisplatin, pemetrexed, pembrolizumab). The patient initially responded well to radiotherapy, with a reduction in tumor size. However, after three months of treatment, there was radiographic progression of left pleural disease and the development of new cervical lymph node metastases.

Six months after the initial diagnosis, a CT-guided biopsy of the left pleura was performed to reassess tumor morphology and explore potential new therapy options. Histologic examination demonstrated well-defined nests of small round cells embedded in desmoplastic stroma (see Table 2 and Figure 3). Abundant apoptotic bodies and areas of necrosis were present. Refer to Table 1 for results of ancillary studies. Molecular testing using fluorescence in situ hybridization (FISH) identified an

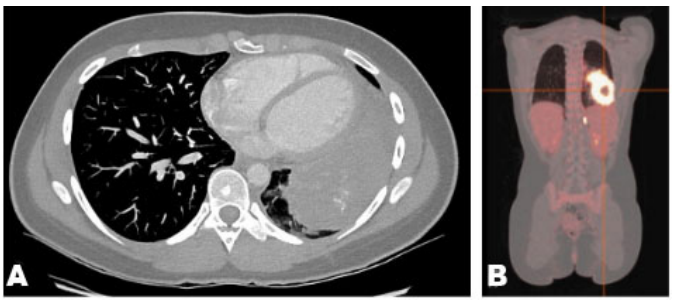

Figure 1: (A) Enhanced computed tomography (CT) of the chest revealed a large, solid mass with central mineralization. The mass showed contiguous involvement of the left pleura, left lower lobe, and left hilum, with compressive effect on adjacent lung tissue. (B) Positron emission tomography (PET) demonstrating intense hypermetabolism with central mineralization and necrosis.

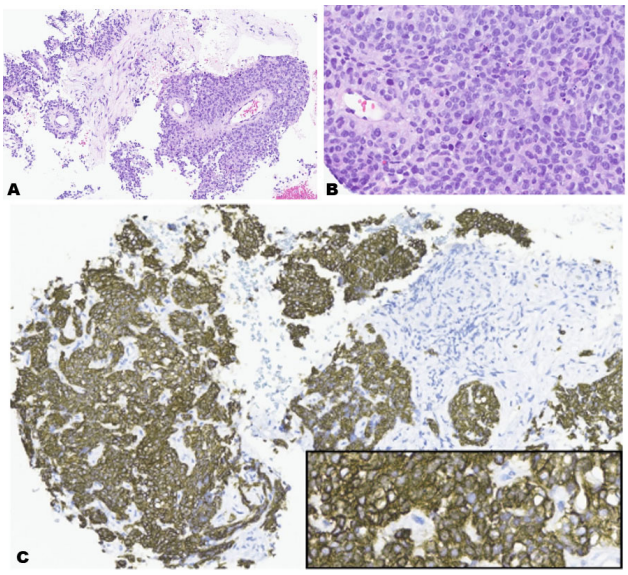

Figure 2: Left lung and mediastinal lymph node biopsies. (A) Densely cellular and well-vascularized fragments of tissue adjacent to fibroblastic stroma (hematoxylin-eosin stain; magnification ×200). (B) Tumor cells showed round to ovoid nuclear contours with indistinct chromatin and scant cytoplasm. Compare nuclear size to intravascular RBCs. Apoptotic bodies were frequent and mitoses were conspicuous (bottom left) (hematoxylin-eosin stain; magnification ×400). (C) Strong and diffuse cytoplasmic immunoreactivity for cytokeratin AE1/AE3 (inset magnification ×400).

EWSR1 rearrangement. Based on the morphological characteristics observed in this biopsy, the diagnosis of desmoplastic small round cell tumor with EWSR1 rearrangement was made.

Following the biopsy, new baseline PET imaging was obtained. This revealed a notable progression of the left pleural disease, characterized by the presence of ring-like and nodular thickening of the pleura that extended into the left infrahilar region. In contrast, there was improvement observed in the characteristics of lung parenchymal involvement, including regional calcification and a reduction in size. These findings were significant

Table 1: Histomorphologic comparison of tumor samplings taken at 0, 6, and 20 months after initial presentation

Sample	Architecture	Nuclei	Cytoplasm	Stroma	Mitotic index	Presence of necrosis
1: EBUS-directed biopsies of mediastinal lymph nodes and left lung	• Densely cellular fragments with abundant vasculature	• Ovoid to round, small to medium size, evenly dispersed chromatin and indistinct nucleoli	Scant	Collagenous, desmoplastic stroma with occasional fibromyxoid areas comprising less than 25% of examined tumor tissue	8–10/10 HPF	• No necrosis (limited/ fragmented sample)
	• Poorly demarcated from surrounding tissue	• Occasional overlapping				• Frequent apoptotic bodies
2: CT-guided pleural biopsy (6 months after sample 1)	• Dense micronodular* nests and cords widely separated by desmoplastic stroma	Similar to Sample 1 with areas of perinuclear clearing	Similar to Sample 1	Collagenous, desmoplastic stroma with frequent fibromyxoid areas comprising at least 70% of examined tumor tissue	<5/10 HPF (post-treatment)	• Eosinophilic, karyorrhectic (coagulative) necrosis centered within nests
	• Less abundant vasculature					• Frequent apoptotic bodies
	• Uninvolved surrounding tissue not identified					
3: Resection of right frontal lobe mass (14 months after sample 2)	• Dense, solid sheets with abundant vasculature	Similar to Sample 1 with some nuclei showing vesicular chromatin	Similar to Sample 1	Absent (tumor nests surrounded by reactive gliosis)	10–12/10 HPF	Similar to Sample 2
	• Relatively well demarcated					

*Micronodules defined as small nests not occupying more than a 10× objective field as described in prior literature [6].
Note: Samples 2 and 3 were obtained after treatment with chemotherapeutics.
Abbreviations: EBUS: Endobronchial ultrasound; CT: Computed tomography; HPF: High power fields.

Table 2: Results of immunohistochemistry (IHC) stains

Stain	Usual staining pattern of DSRCT*	Our case	Pertinent diagnostic differentiation
AE1/AE3	Positive (variable intensity)	Positive (strong/diffuse, cytoplasmic)	
EMA	Positive (variable intensity)	Focally positive (weak, cytoplasmic)	
LMWK	Positive (variable intensity)	Positive (strong/diffuse, cytoplasmic)	
CK5	Negative	Negative	
p40/p63	Negative	Focally positive	
Desmin	Positive (cytoplasmic, dot-like)	Positive (cytoplasmic, dot-like)	
WT1 (N-terminus)	Negative	Negative	Wilms tumor, CIC-DUX4 sarcoma, mesothelioma, rhabdomyosarcoma
WT1 (C-terminus)	Positive (nuclear)	Stain not available	Negative in tumors listed above
Myogenin	Negative	Negative	Rhabdomyosarcoma
Chromogranin	Usually negative (positive in 11%)	Negative	Small cell carcinoma
Synaptophysin	Usually negative (positive in 26%)	Negative	Small cell carcinoma

Table 2: *(Continued)*

Stain	Usual staining pattern of DSRCT*	Our case	Pertinent diagnostic differentiation
CD99	Usually negative, weak if positive	Negative	Ewing sarcoma
CD117 (C-KIT)	Negative (positive in small subset [4, 5])	Negative	Many sarcomas, small cell carcinoma
CD56	Negative	Negative	Small cell carcinoma
CD45	Negative	Negative	Lymphoma
TTF-1	Negative	Negative	Small cell carcinoma
GFAP	Patchy or focal positive [7]	Weakly positive (cytoplasmic)	Gliomas, neuroblastoma
NUT	Negative	Negative	NUT carcinoma and other NUT rearranged neoplasms

*As described by Ordóñez [8].

as they pointed to the pleura as the likely origin site. It is important to note that definitive confirmation could not be attained due to the extensive intrathoracic disease observed during the initial presentation. Therefore, these indirect pieces of evidence were utilized to establish the final diagnosis of pleural DSRCT.

In addition to the progression of pleural disease, there was increased metastatic burden in the mediastinal, left supraclavicular, and left axillary lymph nodes. New lymphadenopathy was observed in the retroperitoneal, gastrohepatic ligament, left common iliac, and left para-aortic regions. Within the limitations of the PET scan, no definite abnormalities were found in the brain.

Treatment was initiated with interval-compressed vincristine, doxorubicin, cyclophosphamide (VAC), alternating with ifosfamide and etoposide (IE), approximately seven months after the patient's initial presentation. To improve patient tolerance, doxorubicin was later alternated with dactinomycin. Repeat imaging after 5 cycles of treatment showed a partial treatment response, but by the 11th cycle, increasing left pleural hypermetabolism on PET imaging indicated early signs of progression. At the final assessment during the 14th cycle, the disease was generally stable, but a persistent metabolic response was observed. The patient was switched to maintenance chemotherapy (vinorelbine/cyclophosphamide) with plans to repeat imaging three months later.

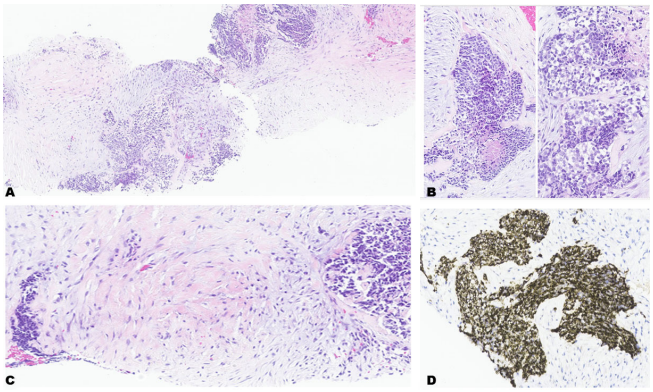

Figure 3: Pleural biopsy. (A) Densely cellular areas widely separated by desmoplastic stroma. (hematoxylin-eosin stain; magnification ×100). (B) Micronodular nests of round, medium size nuclei with evenly dispersed chromatin and indistinct nucleoli. A subset showed perinuclear clearing (right). Necrosis and apoptosis were frequent (hematoxylin-eosin stain; magnification ×250 and ×400). (C) Collagenous, desmoplastic stroma with frequent fibromyxoid areas (hematoxylin-eosin stain; magnification ×250). (D) Strong immunoreactivity for desmin.

Unfortunately, two months into the maintenance treatment (20 months and 14 months after original presentation and DSRCT diagnosis, respectively), the patient was admitted to the hospital with decreased level of consciousness and seizure. She had been experiencing nausea and vomiting for a few days prior to admission. Upon initial assessment, the patient exhibited a fixed and dilated right pupil (6 mm) and a nonreactive left pupil (2 mm). Additionally, there were absent motor responses on the left side. A head CT scan demonstrated a 6 cm intra-axial lesion of the right frontal lobe with 1.2 cm sub-falcine herniation and entrapment of the left lateral ventricle (Figure 4). The patient underwent emergency decompressive craniectomy. Postoperatively the patient had left-sided hemiplegia, dysphagia, and aphasia, and was subsequently transferred to her local facility for ongoing care.

The histologic examination of the resected brain mass revealed large fragments of a well-demarcated, highly cellular neoplasm arranged in compact sheets. Neovascularization and scattered areas of necrosis were observed. Interestingly, there was no apparent presence of desmoplastic stroma surrounding the neoplastic cells. The adjacent brain tissue showed signs of reactive gliosis (see Figures 5 and 6). Refer to Table 1 for the results of the ancillary studies. Reverse transcription–polymerase chain reaction (RT-PCR) performed on the brain mass identified an EWSR1-WT1 fusion with breakpoints at exon 9 of EWSR1 and exon 8 of WT1.

DISCUSSION

The first documentation of pleural-origin DSRCT was published by Bian and colleagues in 1993 [9]. A literature

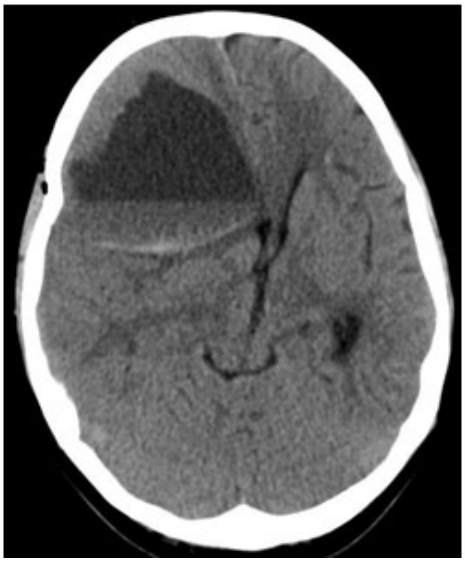

Figure 4: Unenhanced computed tomography showed a large lesion in the right frontal lobe with a fluid–fluid level and layering hemorrhage. Mass effect resulted in right to left sub-falcine herniation and entrapment of the left lateral ventricle.

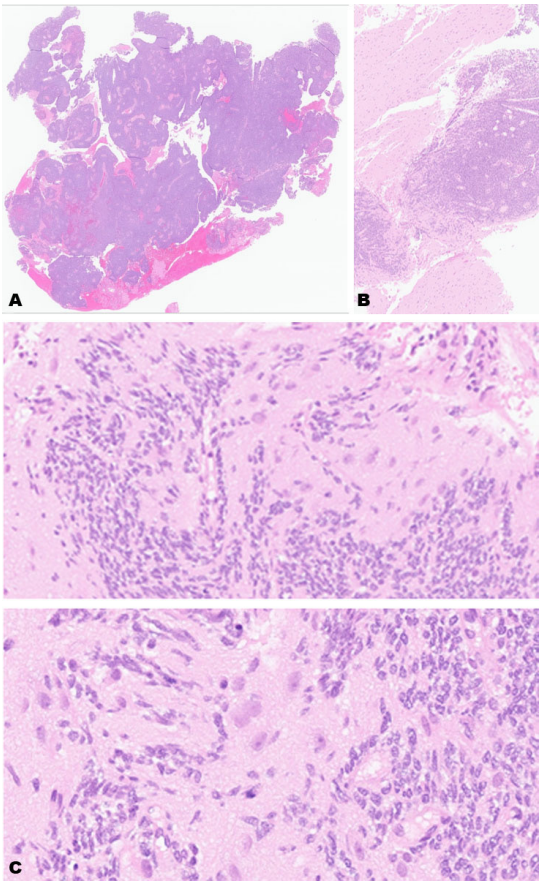

Figure 5: Piecemeal resection of brain mass. (A) Whole slide image of a highly cellular neoplasm with abundant neovascularization. (hematoxylin-eosin stain; magnification ×15). (B) Tumor–brain interface (hematoxylin-eosin stain; magnification ×40). (C) On higher power, tumor cells infiltrated the neural matrix (neurons shown in center of images) in the absence of desmoplastic stroma (hematoxylin-eosin stain; magnifications ×230 and ×400).

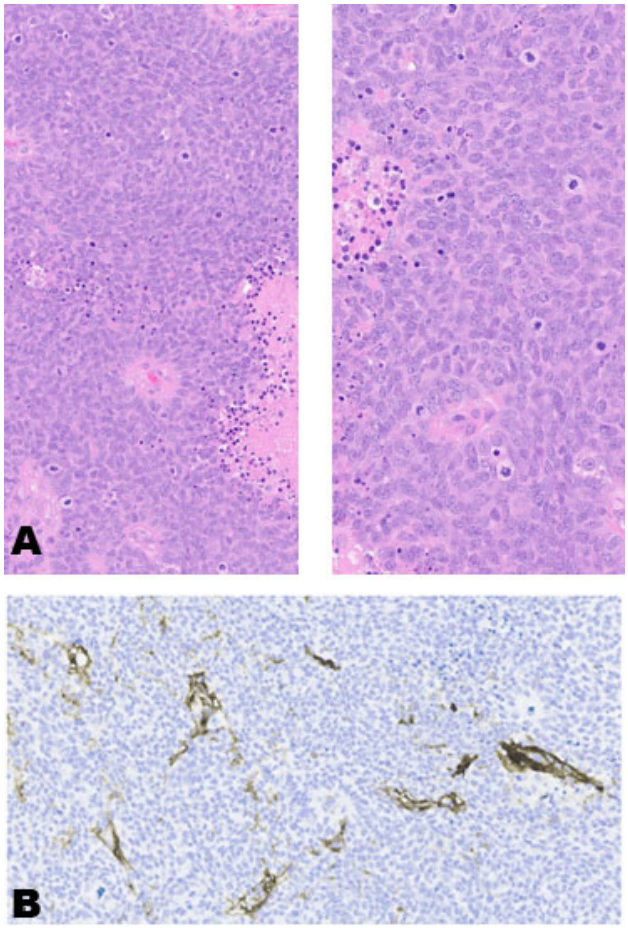

Figure 6: Additional higher power views of the brain mass. (A) (hematoxylin-eosin stain; magnifications ×250 and ×400). (B) Weak, scattered cytoplasmic immunoreactivity for EMA.

review published in 2017 by Fois et al. [10] summarized the findings of previously reported cases of pleural DSRCT in English-language publications, totaling 15 individual cases. The most common presentations included chest pain and pleural effusion, with up to 40% of cases showing involvement of the lungs or mediastinum at the time of diagnosis. Survival beyond three years was low.

This poor survival rate is similar to non-pleural DSRCT cases. A study by Jayakrishnan et al. [11] reviewed their institutional records from 2010 to 2020 and identified seven cases of DSRCT, all males with tumors of typical intra-abdominal origin. All patients presented with gastrointestinal symptoms such as abdominal distention, pain, nausea, and vomiting. Computed tomography imaging revealed widespread peritoneal carcinomatosis in all cases, and two patients had liver metastases at the time of presentation.

The uncommon occurrence of DSRCT in the pleural region may have contributed to delays in receiving appropriate therapy in our case. Similar situations have been reported in the literature, such as the case of a 15-year-old patient with pleural DSRCT who was initially treated for tuberculous pleuritis for two months before the correct diagnosis was made [12].

Our case is not only unique in terms of its site of origin but also appears to be one of the few reported cases in the literature where DSRCT has metastasized non-contiguously to the central nervous system (CNS). This differs from a series of reports that have shown CNS spread from primary CNS DSRCT [6, 13, 14] or cases suggestive of direct extension into the CNS through involvement of spinal nerves [15, 16]. Table 3 provides a summary of DSRCT cases with indirect CNS metastasis available in the literature at the time of review [6, 17–20].

Research investigating the incidence of hematogenous or indirect CNS metastasis from various types of sarcomas indicates a frequency ranging from 0.7% to 3.45%. It has been observed that in the majority of cases, metastasis to the lungs occurs prior to spread to the CNS [21]. Wiens and Hattab [7] conducted a study focusing on general solid tumor metastases in a young population (under 21 years of age) and found that approximately 2.3% of tumors demonstrated CNS metastasis. These metastases often presented as solitary lesions located in the supratentorial space. The average time from diagnosis to CNS spread was 27 months, with a subsequent average survival of 36.6 months.

The literature lacks comprehensive characterization of the morphologic features and clinical presentation of desmoplastic small round cell tumor (DSRCT) metastasis within brain tissue. The case reports listed in Table 3 do not provide details on the examination of lesional tissue, possibly due to the absence of surgical management. Therefore, this case report represents the first histologic description of this uncommon scenario. Table 2 compares the three biopsies performed on this tumor. Allowing for potential therapy-related changes in the second and third specimens, histomorphologic features were largely consistent across these samples: The tumor cells displayed round to ovoid nuclei with vesicular chromatin, indistinct borders, and minimal cytoplasm. Ancillary study results were also concordant. However, the brain metastasis notably lacked desmoplastic stroma, which was evident in the other two biopsies. The absence of clinical history or previous biopsy results would complicate the diagnostic challenge posed by this morphology.

Table 3: Case reports with CNS metastasis from DSRCT of non-CNS origin (indirect/hematogenous spread)

	Author and date	Age, sex, presenting symptoms	Tumor origin	Treatment	Time to CNS spread*	Neurologic symptoms	Neuroimaging features	Outcome
1	Backer et al., 1998 [23]	34, male; supraclavicular lymphadenopathy, cough, night sweats	Unknown	Chemotherapy (VDC/IE), radiation	NS	Intermittent frontal headache	Three hypodense lesions in brain (locations NS)	NS
2	Umeda et al., 2016 [24]	16, male; abdominal pain, weight loss, dyschezia, hematochezia	Pelvic floor	Multiple chemotherapy regimens including VDC/IE, radiation, total resection, PBSCT	14	Headache	One pineal body and three cerebellar lesions, dissemination in CSF	Death 21 months PD (23 months FIS)
3	Al-Ibraheemi et al., 2019 [8]	31, female; NS	Thigh	Unspecified chemoradiotherapy, resection	NS	NS	NS	Alive at publication
4	Jin et al., 2020 [25]	51, male; dyspnea and chest pain	Mediastinum	Chemotherapy (IE), radiotherapy	11	NS	Multiple low density deposits within brain parenchyma (locations NS)	Death 17 months PD
5	Bakhti2022 yar et al., (abstract only) [26]	32, male; progressive paraplegia and urinary retention	Lung	Unspecified chemotherapy	At present -ation	Paraplegia	Diffuse leptomeningeal enhancement	Alive at publication
6	Our case	20, female; cough and rib pain	Pleura	See case history	20	Symptoms of raised ICP (see case)	See case history	Alive at time of writing

*Interval from diagnosis to CNS spread (in months).
Abbreviations: NS: Not specified; VDC/IE: Vincristine, cyclophosphamide, doxorubicin, ifosfamide, etoposide; PBSCT: Peripheral blood stem cell transplant; CSF: Cerebrospinal fluid; PD: Post-diagnosis; FIS: From initial symptoms; ICP: Intracranial pressure.

Lee et al. [22] conducted a study on five cases of primary CNS DSRCT and found that prominent desmoplastic stroma was observed in only two cases. Three out of the five cases exhibited a solid-pattern growth with peripheral entrapment of axons, leading to diagnostic overlap with other primitive CNS neoplasms such as medulloblastoma or astroblastoma. The diagnosis in all five cases was confirmed through genetic evaluation revealing EWSR1-WT1 fusion. The patients were exclusively male, with an age range of 6–25 years and a median age of 11 years. Presenting symptoms included seizures, headaches, numbness, and weakness. Four tumors were located supratentorially, while one was located in the posterior fossa. Magnetic resonance imaging findings varied from heterogeneously enhancing masses with a small cystic component to predominantly cystic masses with solid enhancing nodules. Other accounts of primary CNS DSRCT describe the stroma as varying in its presence, ranging from minimal [23] to abundant [13, 14, 24], predominantly collagenous but also described as fibromyxoid [25].

Desmoplastic small round cell tumor demonstrating a solid pattern without desmoplastic stroma has been described as a variant pattern by Ali et al. [26] in a case report of an adolescent female with intra-abdominal DSRCT. However, no subsequent tissue sampling was reported. Similarly, Al-Ibraheemi et al. [6] found the absence of desmoplasia in 6 out of 34 primary DSRCT specimens, all of which exhibited a solid pattern morphology. It is unlikely that the nature of the CNS environment was responsible for the loss of desmoplastic stroma in the CNS, as many metastatic CNS lesions of different lineages (epithelial, mesenchymal, and neuroendocrine) are associated with this feature [27]. It is understandable that primary tumors lacking desmoplasia can present a diagnostic challenge as they may resemble other “small round cell” neoplasms such as Ewing sarcoma, rhabdomyosarcoma, small cell carcinoma, or lymphoma. In such cases, the use of immunohistochemical studies can help narrow down the differential diagnosis, while molecular confirmation of the EWSR1-WT1 fusion provides further identification. It should be noted that the EWSR1-WT1 fusion has been documented in neoplasms other than DSRCT [28–30] and therefore must be interpreted in the context of the clinical history and histopathologic features of each case.

CONCLUSION

This case report presents a rare occurrence of DSRCT with hematogenous metastasis to the central nervous system in a young female with a pleural-origin tumor. As expected from the aggressive nature of this tumor group, our case exhibited local spread at the time of presentation. Due to delays in reaching a definitive diagnosis, the patient initially received lung cancer chemotherapeutics before transitioning to the standard VAC/IE treatment. Subsequent spread to the right frontal lobe led to significant neurological impairment and residual deficits on the left side. Recognizing the typical histomorphology of DSRCT and maintaining a high suspicion for alternative diagnoses in young non-smokers presenting with advanced thoracic disease are crucial in the initial identification of this rare entity. Conducting appropriate histological and immunohistochemical evaluations, followed by molecular confirmation of EWSR1-WT1 fusion, can help rule out mimicking conditions such as undifferentiated carcinoma, lymphoma, and other small round cell tumors.

Finally, our case represents the first detailed description of the distinctive morphological characteristics of a metastatic DSRCT within the brain, including the observed stromal heterogeneity between the primary and metastatic sites. Further literature is needed to fully define the histological spectrum of this entity.

REFERENCES

1. Gerald WL, Rosai J. Case 2. Desmoplastic small cell tumor with divergent differentiation. Pediatr Pathol 1989;9(2):177–83.
2. WHO Classification of Tumours Editorial Board, editor. Soft Tissue and Bone Tumours: WHO Classification of Tumours. 5ed. Geneva: World Health Organization Publications; 2020.
3. Gerald WL, Miller HK, Battifora H, Miettinen M, Silva EG, Rosai J. Intra-abdominal desmoplastic small round-cell tumor. Report of 19 cases of a distinctive type of high-grade polyphenotypic malignancy affecting young individuals. Am J Surg Pathol 1991;15(6):499–513.
4. Fine RL, Shah SS, Moulton TA, et al. Androgen and c-Kit receptors in desmoplastic small round cell tumors resistant to chemotherapy: Novel targets for therapy. Cancer Chemother Pharmacol 2007;59(4):429–37.
5. Zhang PJ, Goldblum JR, Pawel BR, Fisher C, Pasha TL, Barr FG. Immunophenotype of desmoplastic small round cell tumors as detected in cases with EWS-WT1 gene fusion product. Mod Pathol 2003;16(3):229–35.
6. Al-Ibraheemi A, Broehm C, Tanas MR, et al. Desmoplastic small round cell tumors with atypical presentations: A report of 34 cases. Int J Surg Pathol 2019;27(3):236–43.
7. Wiens AL, Hattab EM. The pathological spectrum of solid CNS metastases in the pediatric population. J Neurosurg Pediatr 2014;14(2):129–35.
8. Ordóñez NG. Desmoplastic small round cell tumor: I: A histopathologic study of 39 cases with emphasis on unusual histological patterns. Am J Surg Pathol 1998;22(11):1303–13.
9. Bian Y, Jordan AG, Rupp M, Cohn H, McLaughlin CJ, Miettinen M. Effusion cytology of desmoplastic small round cell tumor of the pleura. A case report. Acta Cytol 1993;37(1):77–82.
10. Fois AG, Pirina P, Arcadu A, et al. Desmoplastic small round cell tumors of the pleura: A review of the clinical literature. Multidiscip Respir Med 2017;12:22.

11. Jayakrishnan T, Moll R, Sandhu A, Sanguino A, Kaur G, Mao S. Desmoplastic small round-cell tumor: Retrospective review of institutional data and literature review. Anticancer Res 2021;41(8):3859–66.
12. Jian Z, Shaohong H, Wenzhao Z, Lijia G. Misdiagnosed desmoplastic small round cell tumor of the pleura: Case report and literature review. J Formos Med Assoc 2014;113(1):60–1.
13. Thondam SK, du Plessis D, Cuthbertson DJ, et al. Intracranial desmoplastic small round cell tumor presenting as a suprasellar mass. J Neurosurg 2015;122(4):773–7.
14. Neder L, Scheithauer BW, Turel KE, et al. Desmoplastic small round cell tumor of the central nervous system: Report of two cases and review of the literature. Virchows Arch 2009;454(4):431–9.
15. Ray R, Traunecker HC, Raafat F, Stevens MC. Desmoplastic small round cell tumour of childhood: A report of four cases demonstrating wider clinical features and variable outcome. Sarcoma 1997;1(2):103–8.
16. Cacciotti C, Samji N, Cox S, et al. Desmoplastic small round cell tumor with ascending intraspinal metastasis at recurrence: Case report and review of the literature. J Pediatr Hematol Oncol 2022;44(2):e561–6.
17. Backer A, Mount SL, Zarka MA, et al. Desmoplastic small round cell tumour of unknown primary origin with lymph node and lung metastases: Histological, cytological, ultrastructural, cytogenetic and molecular findings. Virchows Arch 1998;432(2):135–41.
18. Umeda K, Saida S, Yamaguchi H, et al. Central nervous system recurrence of desmoplastic small round cell tumor following aggressive multimodal therapy: A case report. Oncol Lett 2016;11(1):856–60.
19. Jin D, Chen M, Wang B, Gou Y. Mediastinal desmoplastic small round cell tumor. Medicine (Baltimore) 2020;99(44):e22921.
20. Bakhtyar M, Oviedo S, Bhatti S. A rare case of desmoplastic small round cell tumor with leptomeningeal carcinomatosis. Chest 2022;161(6 Suppl):A325.
21. Bekiesinska-Figatowska M, Duczkowska A, Duczkowski M, et al. CNS metastases from bone and soft tissue sarcomas in children, adolescents, and young adults: Are they really so rare? Biomed Res Int 2017;2017:1456473.
22. Lee JC, Villanueva-Meyer JE, Ferris SP, et al. Clinicopathologic and molecular features of intracranial desmoplastic small round cell tumors. Brain Pathol 2020;30(2):213–25.
23. Lopez-Nunez O, Cafferata B, Santi M, et al. The spectrum of rare central nervous system (CNS) tumors with EWSR1-non-ETS fusions: Experience from three pediatric institutions with review of the literature. Brain Pathol 2021;31(1):70–83.
24. Tison V, Cerasoli S, Morigi F, Ladanyi M, Gerald WL, Rosai J. Intracranial desmoplastic small-cell tumor. Report of a case. Am J Surg Pathol 1996;20(1):112–7.
25. Bouchireb K, Auger N, Bhangoo R, et al. Intracerebral small round cell tumor: An unusual case with EWS-WT1 translocation. Pediatr Blood Cancer 2008;51(4):545–8.
26. Ali A, Mohamed M, Chisholm J, Thway K. Solid-pattern desmoplastic small round cell tumor. Int J Surg Pathol 2017;25(2):158–61.
27. Chang KC, Lu YC, Lin MJ, Chen HY, Jin YT. Desmoplastic tumour-associated stroma versus neural tissue in central nervous system metastasis: Effects of different microenvironments on tumour growth. Histopathology 2011;59(1):31–9.
28. Alaggio R, Rosolen A, Sartori F, et al. Spindle cell tumor with EWS-WT1 transcript and a favorable clinical course: A variant of DSCT, a variant of leiomyosarcoma, or a new entity? Report of 2 pediatric cases. Am J Surg Pathol 2007;31(3):454–9.
29. Ud Din N, Pekmezci M, Javed G, et al. Low-grade small round cell tumor of the cauda equina with EWSR1-WT1 fusion and indolent clinical course. Hum Pathol 2015;46(1):153–8.
30. Schoolmeester JK, Folpe AL, Nair AA, et al. EWSR1-WT1 gene fusions in neoplasms other than desmoplastic small round cell tumor: A report of three unusual tumors involving the female genital tract and review of the literature. Mod Pathol 2021;34(10):1912–20.

****

Author Contributions

Rebecca Phillips – Conception of the work, Design of the work, Acquisition of data, Analysis of data, Interpretation of data, Drafting the work, Final approval of the version to be published, Agree to be accountable for all aspects of the work in ensuring that questions related to the accuracy or integrity of any part of the work are appropriately investigated and resolved

Sumit Das – Conception of the work, Design of the work, Acquisition of data, Analysis of data, Drafting the work, Revising the work critically for important intellectual content, Final approval of the version to be published, Agree to be accountable for all aspects of the work in ensuring that questions related to the accuracy or integrity of any part of the work are appropriately investigated and resolved

Guarantor of Submission

The corresponding author is the guarantor of submission.

Source of Support

None.

Consent Statement

Written informed consent was obtained from the patient for publication of this article.

Conflict of Interest

Authors declare no conflict of interest.

Data Availability

All relevant data are within the paper and its Supporting Information files.